[Article ID] 1003- 6326(2001)04- 0583- 04

Density functional calculation of equilibrium geometry and electronic structure of pyrite①

QIU Guan-zhou(邱冠周), XIAO Qi(肖 奇), HU Yue-hua(胡岳华), XU Jing(徐 竞)
(Department of Mineral Processing, Central South University,
Changsha 410083, P. R. China)

[Abstract] The equilibrium geometry and electronic structure of pyrite has been studied using self-consistent density-functional theory within the local density approximation (LDA). The optimum bulk geometry is in good agreement with crystallographic data. The calculated band structure and density of states in the region around the Fermi energy show that valence-band maximum (VBM) is at X (100), and the conduction-band minimum (CBM) is at G (000). The indirect and direct band gaps are 0.6 eV and 0.74 eV, respectively. The calculated contour map of difference of charge density shows excess charge in nonbonding d electron states on the Fe sites. The density increases between sulfur nuclei and between iron and sulfur nuclei qualitatively reveal that S—S bond and Fe—S bond are covalent binding.

[Key words] density functional calculation; electronic structure; equilibrium geometry; pyrite
[CLC number] O 471.5; P 578.292 [Document code] A

1 INTRODUCTION

Pyrite (FeS_2) is a typical 3d transition metal material. A comprehensive study of electronic structure of FeS_2 is helpful to understanding the series of electronic structure of transition metal disulfide MS_2 (M= Fe, Co, Ni, Cu, Zn) with the pyrite structure because of their wide range of electric, magnetic and optical properties. Recently, much interest has focused on pyrite for its promising capabilities as a material for photovoltatic application[1]. This is related to the high quantum efficient (> 90%) and the high absorption coefficient (> 10^5 cm^{-1} for $h\upsilon$> 1.3 eV), but also benefits from the nontoxicity of the constituents. In addition, pyrite is one of the most abundant sulfide minerals. Pyrite oxidation or dissolution in aqueous solution is of particular significance to such various engineering application as eletrochemistry of sulfide flotation[2], bio-leaching of low-grade chalcopyrite-containing ore[3], coal processing, environmental engineering, geochemistry. In recent years, semiconductor electrochemistry of sulfide minerals has wide applications in the interpretation of sulfide oxidation or dissolution[4]. Any study of the electrochemistry of sulfide minerals must take into account the influence of the electronic structure of sulfide minerals.

Although a lot of experimental[5] and theoretical[6] work has been performed on the pyrite, there are still distinct discrepancies concerning the exact shape of the bands and band gap. In particular, the upper valence and lowest conduction bands of pyrite and hence the location of the valence band maximum and conduction band minimum are not yet fully resolved. In addition, the pyrite structure has two structural degrees of freedom, namely the lattice constant a_0 and the Wyckoff X_s determining the positions of the sulfur atoms in the unit cell. Theoretical values of these parameters have been published in a recent paper[7], further theoretical studies of them have, to our knowledge, not been published yet.

In this paper, we use the ab initio calculation methods based on density functional theory to study the equilibrium geometry, electronic structure feature, energy band structure, and electron density of pyrite.

2 METHODS OF CALCULATION

The calculation methods used in this work are based on density-functional theory (DFT)[8] within the local density approximation (LDA)[9], implemented using norm-conserving pseudo-potentials[10] and a mixed-basis representation of the electronic wave functions. First-principle, norm-conserving pseudo-potentials in Kleinman-Bylander representation were generated using the optimization scheme of Lin et al[10] in order to reduce the required value of the plane-wave cut-off E_{cut}. The calculations have been done using a plane wave cut-off 600 eV for FeS_2. Our tests show that with this cut-off the energy per unit cell is converged to within 0.000 01 eV. The present calculations are performed with the CASTEP (Cambridge Serial Total Energy Package)

① [Foundation item] Project (59925412) supported by the National Science Funding for Distinguished Young Scholars
[Received date] 2000- 09- 28; [Accepted date] 2001- 01- 05

code and its parallel version CETEP (Cambridge-Energy total energy package).

The CASTEP package is capable of simulating electronic relaxation to ground state for metals, insulators, or semiconductors. Using these techniques, CASTEP can calculate forces acting on atoms and stress on the unit cell. Atomic forces can be used to find the equilibrium structure.

Crystal structure of FeS_2 used in the calculation is presented as follows. At room temperature FeS_2 crystallizes within the cubic space group T_h^6– Pa3, Z = 4, as shown in Fig. 1(a). The local coordination of the iron atoms is sixfold and the sulfur atoms are fourfold. Fe atoms are coordinated to six sulfur atoms, which have bonds to three Fe atoms and to one S atom. The experimentally determined cubic lattice constant a_0 is 0.5416 nm and the nearest distance between S sites d_{S-S} is 0.216 nm[5]. Its corresponding irreducible wedge of the Brillouin zone is shown in Fig. 1(b).

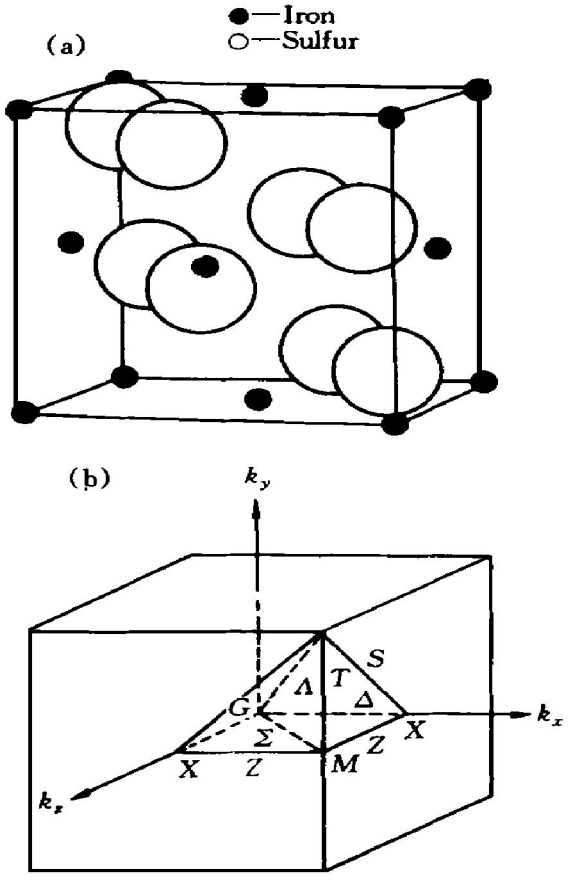

Fig. 1 Crystal structure of pyrite (a) and Brillouin zone (b)

3 RESULTS AND DISCUSSION

3.1 Structure optimization

The pyrite structure has two degrees of freedom: the lattice constant a_0 and a parameter X_s, which determines the nearest S—S distance d_{S-S}. A search in this two-dimensional parameter space is made to determine the optimal geometry of the material. The results of the search are summarized in Table 1. Our results are in excellent agreement with the experimental data (as shown in Fig. 1).

Table 1 Summary of geometry optimization for pyrite

Item	a_0 / nm	X_s	d_{S-S} / nm	d_{Fe-S} / nm	B / GPa
Theoretical	0.53823	0.38456	0.2144	0.2249	154.32
Experimental	0.5416	0.385	0.2162	0.2269	145
Deviation/%	– 0.6	– 0.2	– 0.2	– 0.9	+ 6

3.2 Calculation of energy-band structure and density of states

The calculations of the electronic structure have been conducted using the experimental lattice parameters. In Figs. 2 and 3 the calculated band structure of FeS_2 is shown along the selected high symmetry lines and the corresponding density of states. These results are in good agreement with the recently published calculations by Eyert et al[11]. The band structure is split into five groups of bands in the range between – 16 eV and 5 eV. It can be described in terms of states of S_2^{2-} molecular ions (3s σ, pair 3s σ*, 3p σ, 3p π, 3p π* and 3p σ*) and of crystal-field split 3d states of Fe^{2+} (e_g and t_{2g}). The lowest two bands near – 15 eV and – 10 eV are well described by the bonding and antibonding of molecular states 3s σ and 3s σ*.

The band of states between – 6 eV and 0 eV can be described as a mixed of states derived from molecular states 3p σ, 3p π, 3p π* and a small part of bonding of the Fe e_g state. The narrow band just below the Fermi level is primarily the nonbonding Fe t_{2g} state.

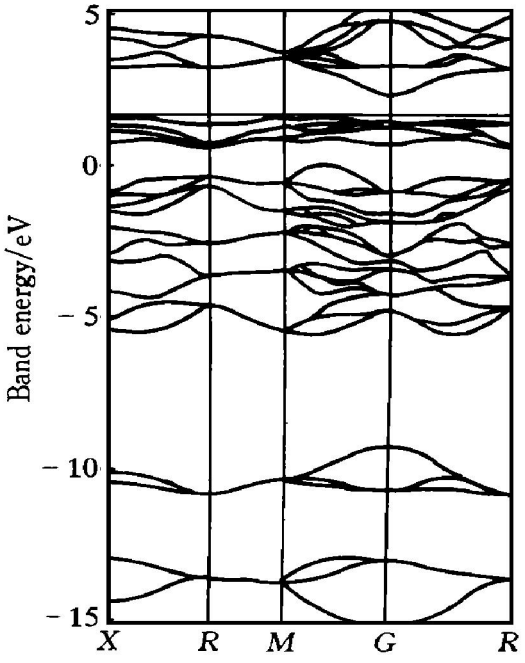

Fig. 2 Band structure of pyrite calculated with experimental lattice parameters

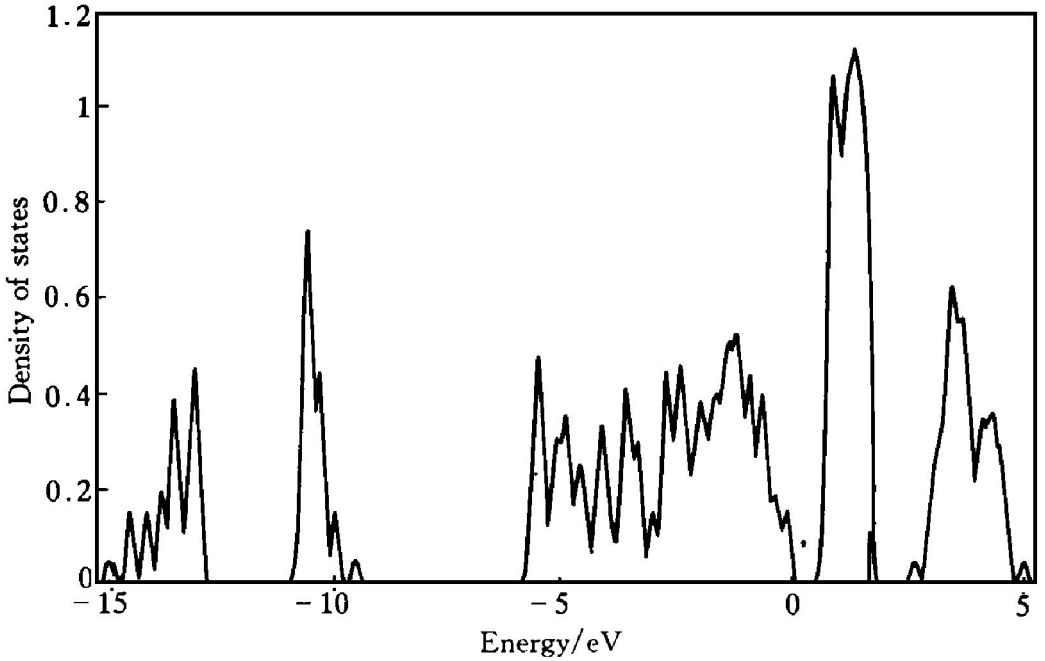

Fig. 3 Density of states of pyrite calculated with experimental lattice parameters

Finally, the unoccupied band above the Fermi levels corresponding mixture of the antibonding molecular $3p\sigma^*$ state and the Fe e_g states.

Fig. 4 shows the extended region around the Fermi energy from Fig. 2, which makes details of the highest valence band and lowest conduction band apparent. Pyrite is predicted to be a relatively narrow band-gap semiconductor. The valence-band maximum is at X (100), and the conduction-band minimum is at G (000). The indirect band gap between these two points is calculated to be 0.6 eV, the smallest direct gap is found to be 0.74 eV. The calculated optical band gap, which compares well with the gap of 0.59 eV obtained by Zhao et al[12], 0.68 eV by Ahuja et al[13] and 0.7 eV by Folkerts et al[14], is smaller than the experimental values. The experimental situation is unclear concerning the size of the gap, with measured values ranging from 0.7 eV to 2.62 eV and it is thought that these variations can be explained by the fact that most experiments were performed on pyrite samples obtained from mines. Since each sample had a different level of impurity concentration, this could be one of the reasons for the large variation in the values of the measured energy gap. Nevertheless, it should be pointed out that density functional theory, being a ground state theory, is not intended to properly account for the size of the optical band gap. Still, the tendency of the LDA is to underestimate the optical band gap.

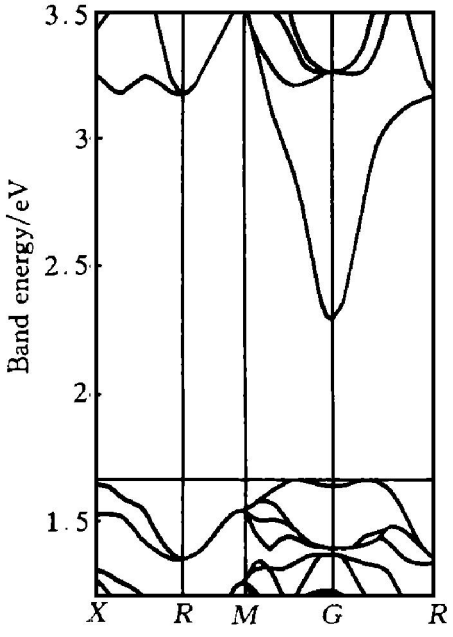

Fig. 4 Band structure of pyrite around Fermi energy

3.3 Valence electron density and chemical binding

The results for the spatial distribution of electron density (actually the pseudo-density) is shown in Fig. 5. The charge on the Fe lattice shows spherical distribution. It is clear that charge distribution centered on the Fe site must consist mainly of 3d electrons, also.

In order to analyze the density in more detail, the charge density difference has been calculated, which is defined to be the result of the electron density in the solid minus the density of superposed spherical atoms. A contour plot of the charge density difference is shown in Fig. 6. According to the shape of the charge density difference, it is possible to draw the following qualitative conclusions. The density near the Fe sites shows a buildup of charge in t_{2g} (nonbonding) states at the expense of charge in the e_g states. There is also a buildup of charge at the midpoint of both S—S bond and the Fe—S bond.

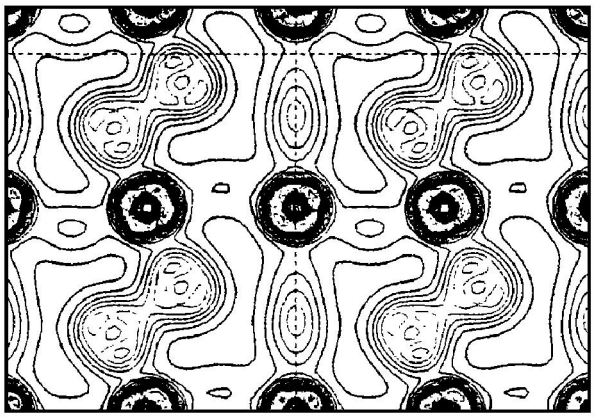

Fig. 5 Contour plot of valence electron pseudodensity on (110) plane passing through Fe and S sites

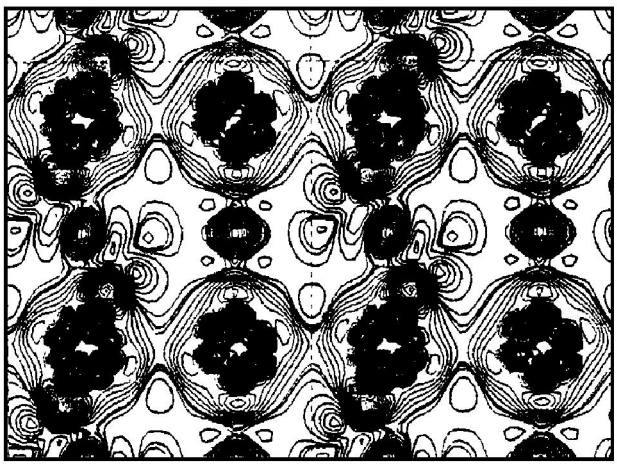

Fig. 6 Contour plot of charge density difference on (110) plane passing through Fe and S sites

4 CONCLUSIONS

In the present work, we have performed equilibrium geometry and electronic structure calculation using self-consistent density-functional theory within local-density-approximation (LDA). The calculated lattice constant, sulfur parameter and bulk modulus in a typical LDA are in agreement with experimental values. The calculated band structure is consistent with recent calculations. Although the calculated gap is smaller than the experimental value, it may be reliable that the gap is indirect and that the highest valence-band maximum and lowest conduction-band minimum are located at $X(100)$ and $G(000)$, respectively. Meanwhile, our charge density calculation shows a direct physical picture of chemical binding.

Moreover, based on the success of understanding the electronic structure of the stoichiometric pyrite, the CASTEP package based on DFT-pseudopotential methods is extended to treat the defect problems, such as point defects in nonstoichiometric FeS_{2-x}, dislocation and surface of FeS_2. Therefore, the relation between electronic structure of defect crystal and chemical reactivity can be comprehensively understood so that the oxidation of FeS_2 during the processing and application of the ultrafine pyrite can be effectively controlled.

[REFERENCES]

[1] Ennaoui A, Fiechter S, Jaegermann W, et al. Photoelectrochemistry of highly quantum efficient single-crystalline n-FeS_2(pyrite) [J]. J Electrochem Soc, 1986, 133(1): 97- 106.

[2] HU Yue-hua, QIU Guan-zhou, SUN Shui-yu, et al. Recent development in researches of electrochemistry of sulfide flotation at Central South University of Technology [J]. Trans Nonferrous Met Soc China, 2000, 10 (Special Issue): 1- 7.

[3] QIU Guan-zhou, WANG Jun, HU Yue-hua, et al. Bioleaching of low-grade large porphyry chalcopyrite-containing ore [J]. Trans Nonferrous Met Soc China, 2000, 10 (Special Issue): 19- 22.

[4] CHEN Jian-hua, FENG Qi-ming, LU Yi-ping. Energy band model of electrochemical flotation and its application (I): Theory and model of energy band of semiconductor solution interface [J]. The Chinese Journal of Nonferrous Metals, 2000, 10(2): 240- 244.

[5] Daid J, Vanhan R, Craig J. Mineral Chemistry of Metal Sulfides [M]. Cambridge, 1978. 36- 38.

[6] Lauer S, Trautwein A X, Harris F E. Electronic-structure calculation, photoelectron spectra, optical spectra, and Mosbuer parameters for the pyrites MS_2 (M = Fe, Co, Ni, Zn) [J]. Physical Review B, 1984, 29(12): 6774- 6783.

[7] Opahle I, Koepernik K, Schrig H E. Full-potential band-structure calculation of iron-pyrite [J]. Physical Review B, 1999, 60(20): 14035- 14041.

[8] Kohn W, Sham L J. Self-consistent equations including exchange and correlation effects [J]. Physical Review A, 1965, 140(4): 1133- 1138.

[9] Perdew J P, Zunger A. Self-interaction to density-functional approximations for many-electron systems [J]. Physical Review B, 1981, 23(10): 5048- 5079.

[10] Lin J S, Qteish A, Payne M C, et al. Optimized and transferable nonlocal separable ab initio pseudopotentials [J]. Physical Review B, 1993, 47(8): 4174- 4180.

[11] Eyert V, Hock K H, Fiechter S, et al. Electronic structure of FeS_2: The crucial role of electron-lattice interaction [J]. Physical Review B, 1998, 57(11): 6350 - 6359.

[12] Zhao G L, Callaway J, Hayashibara M. Electronic structure iron and cobalt pyrites [J]. Physical Review B, 1993, 48: 15781- 15786.

[13] Ahuja R, Eriksson O, Johansson B. Electronic and optical properties of FeS_2 and CoS_2 [J]. Philosophical Magazine B, 1998, 78(5/6): 475- 480.

[14] Folkerts W, Sawatzky G A, Haas C, et al. Electronic structure of 3D transition-metal pyrites [J]. J Phys C: Solid State Phys, 1987, 20: 4135- 4144.

(Edited by HE Xue-feng)